Seismic Imaging of Deep Mantle Discontinuities

B. Tauzin, E. Debayle, G. Wittlinger, C. Zaroli,

Ecole et Observatoire de Sciences de la Terre, Centre National de la Recherche Scientifique and Université Louis Pasteur,
5 rue René Descartes, 67084 Strasbourg Cedex, France.

benoit.tauzin@eost.u-strasbg.fr

Ecole et Observatoire des Sciences de la Terre

Financé par ANR

ulp UNIVERSITÉ LOUIS PASTEUR STRASBOURG

Summary

The Earth reflectivity reveals deep seismic discontinuities at 410 and 660 km depths which are often interpretated as pressure-induced phase-transformations of the olivine mineral, a major constituent of the mantle. It has been shown that the depth of these discontinuities is temperature dependent. The mantle transition zone (the MTZ, the part of the mantle lying between the two discontinuities) could give some insights on the nature of exchanges between lower and upper mantle.

We process teleseismic records (**figure 1**) of earthquakes at 3-components broad-band seismological stations distributed all over the world**.** As it may be done in oil exploration, we derive the absolute discontinuity depths from the analysis of travel-times of reflected and converted waves at these discontinuities (**figures 2** and **3**).

P-to-S conversions give constraints on the structure under the receiver (**figure 2 left**). To enhance conversion energy on seismograms, we apply a receiver-function technique which consists on deconvolving the P-wave energy from the Sv component (**figure 3 left**).

Underside reflections of shear-waves are more sensitive to the structure under bounce points between the seismic source and the receiver and enable a better coverage of oceanic regions (**figure 2 right**).

Conversion data are gathered by receivers (**figures 3, 4 left**) and reflection data by common bounce points (**figures 3, 4 right**). Weak converted/reflected phases are then enhanced by stacking in the time-slowness domain the records having the highest signal to noise ratio (**figure 5**).

We finally use a radial velocity model to convert our travel-time measurements into absolute depth of discontinuities.

We present our observations of perturbations of the MTZ thickness (**figure 6 left**). We show that these perturbations are partly correlated with expected locations of downwelling of cold subducted material from the surface (**figure 6 right**).

Broad-Band Seismic Records

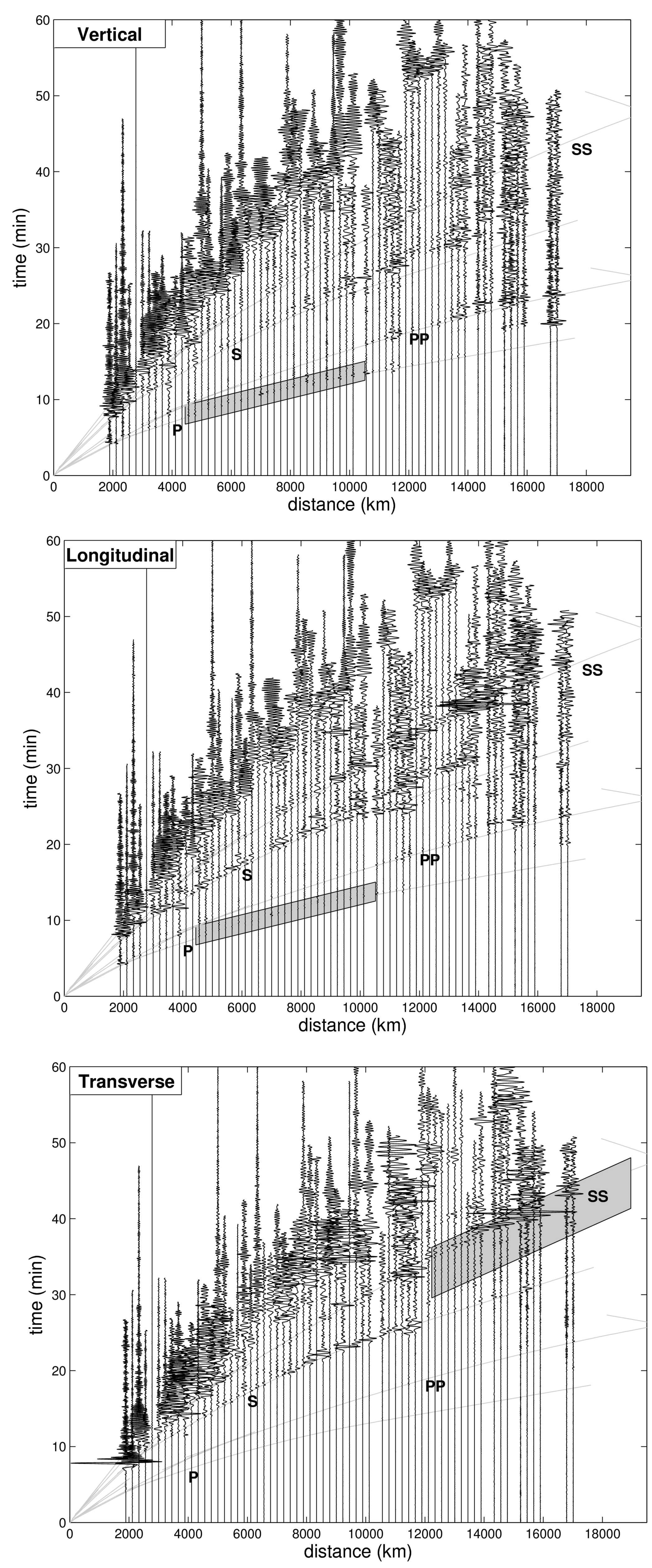

Figure 1. High quality seismic sections for the broad-band seismological station CAN (Canberra, Australia), over the period 1997-2006. Several seismic phases have been emphasized (P, PP, S and SS). The P shaded boxes on the vertical and longitudinal sections correspond to analysed time and distance windows for the study of P-to-S conversions. The SS shaded box on the transverse section correspond to the analysed time and distance window for the study of SS-precursors.

Ray Geometry

P-to-S conversions | SS-precursors

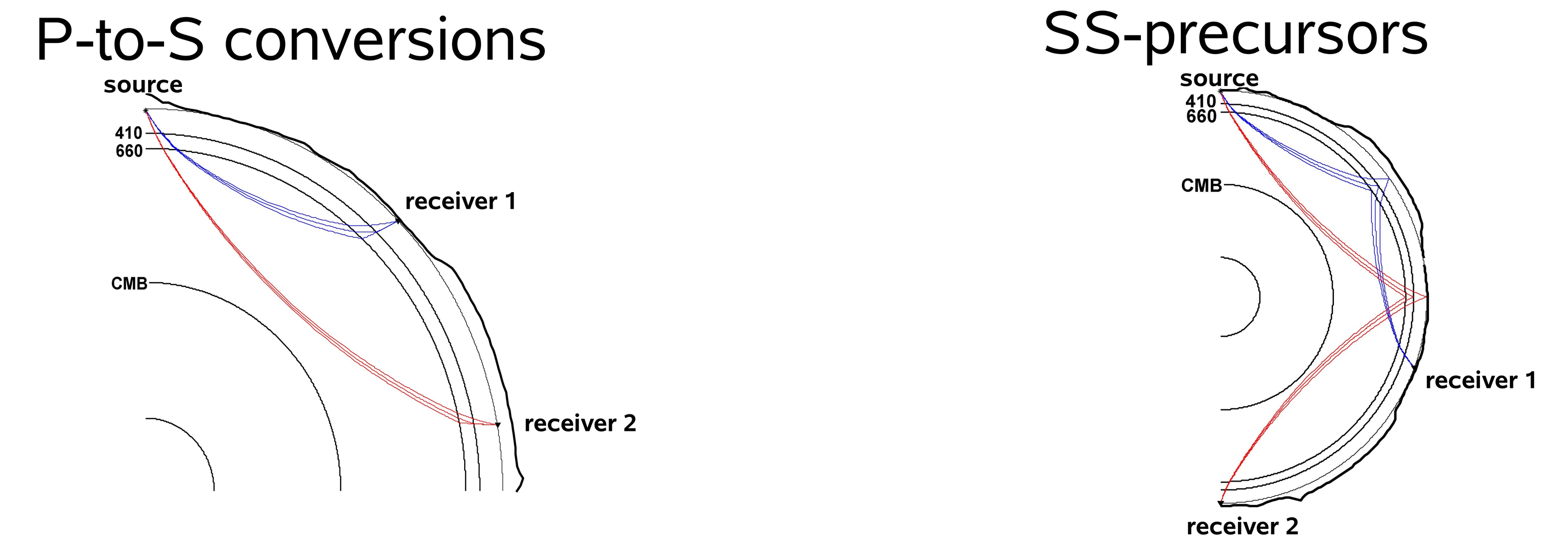

Figure 2. Earth slices with major structural discontinuities (410: the 410-km discontinuity, 660: the 660-km discontinuity, CMB: the Core-Mantle Boundary). Left: Ray paths for P-to-S conversions under receivers. Right: Ray paths for SS-precursors with bounce points at mid-distance between source and receivers.

Earth reflectivity

P-to-S conversions | SS-precursors

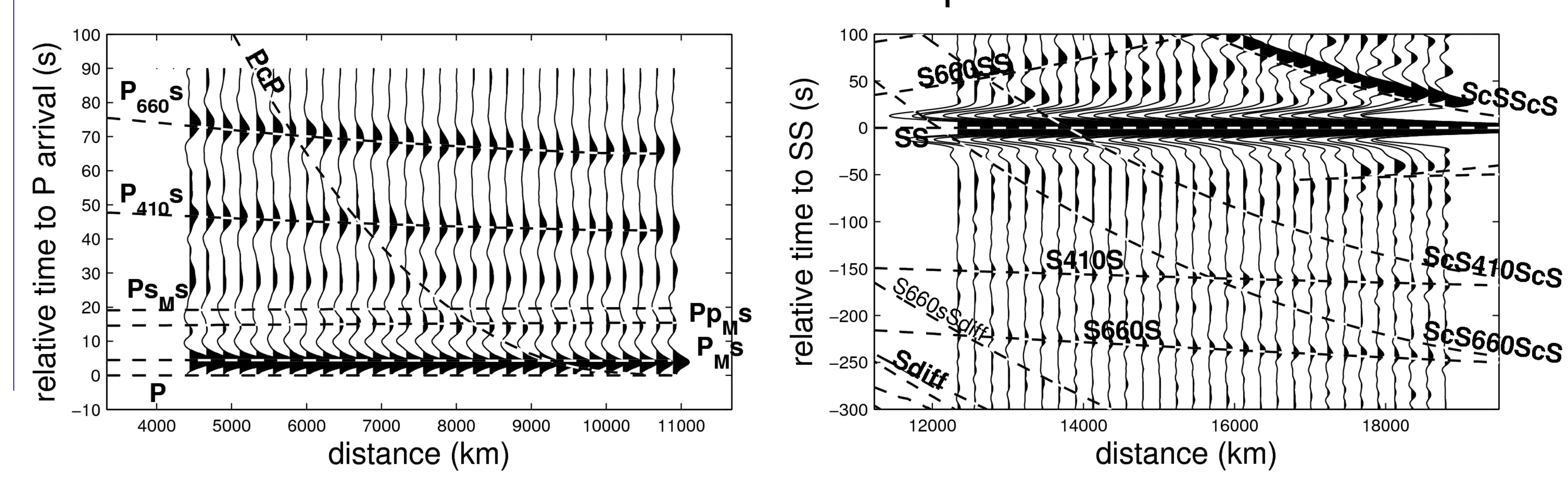

Figure 3. Seismic sections corresponding to P and SS boxes on **figure 1** for global conversion and reflection data sets. Left: P-to-S conversions at discontinuities ($P_{410}s$ and $P_{660}s$) are better recorded between 40° and 97° and arrive ~45 s and ~70 s after P direct arrival. Right: Underside reflections of S phases at discontinuities (S410S and S660S) are better recorded between 110° and 170° and arrive ~-155 s and ~-230 s before SS (as precursors).

Earth coverage

P-to-S conversions | SS-precursors

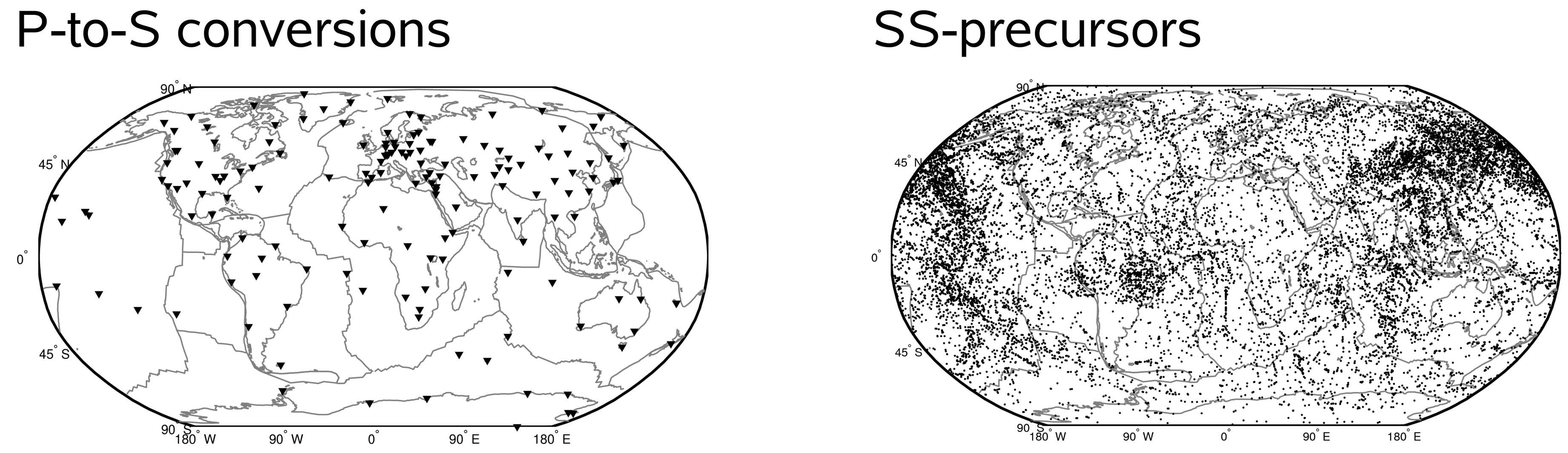

Figure 4. Maps of data coverage. Before stacking, conversion data are gathered by receivers (162 stations, left) and reflection data by common SS bounce points (17578 bounce points in 362 cells, right).

Stacking

P-to-S conversions | SS-precursors

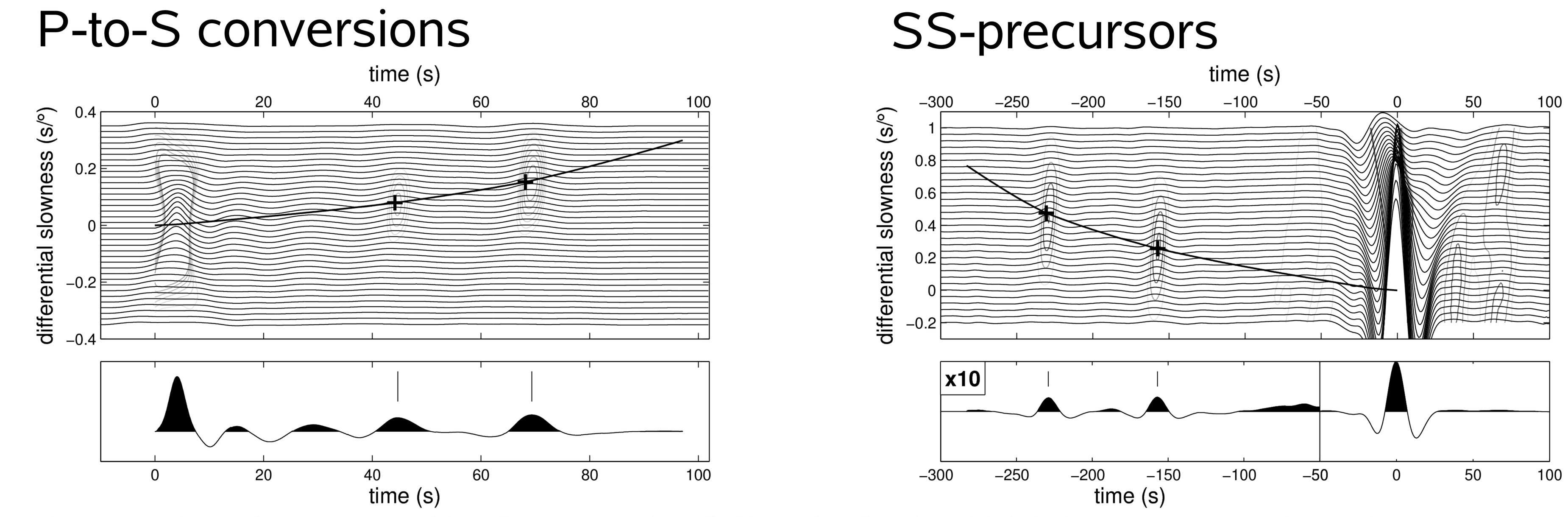

Figure 5. Time-slowness stacking for conversion (left) and reflection (right) data sets. At each receiver or cap location, a stacked seismic trace (bottom) is built from the amplitudes along the theoretical time and slowness values for a radial velocity model and a reference epicentral distance (black curves on top time-slowness diagrams). We then measure arrival times of converted and reflected waves relative to their respective reference waves.

Insights on geodynamics

MTZ Thickness

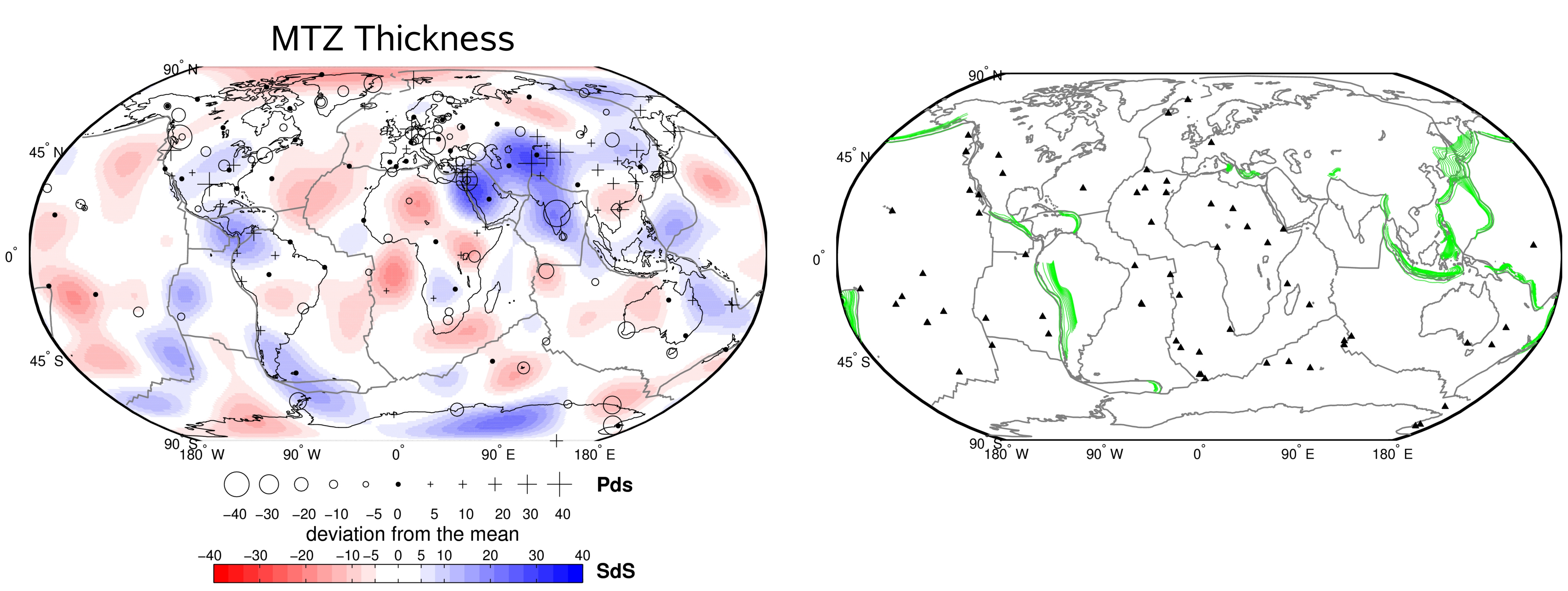

Figure 6. Left: Variations of the MTZ thickness relative to the global average. A radial velocity model was used to convert travel-times into depths. P-to-S conversion observations are marked by black crosses (> 5 km), black dots (~0 km) and black circles (< -5 km). Background colors represent SS-precursors observations which cover the entire surface of the Earth. Blue represents thicker observations, red thinner observations. Right: Geographical locations of hotspots (black triangles) and major subduction zones (green).

Acknowledgements

This work was supported by the program DyeTI of the Institut National des Sciences de l'Univers (INSU) at CNRS and by young researcher ANR TOMOGLOB no ANR-06-JCJC-0060. We thank the IRIS and Geoscope data centers for providing seismological data.